Available online at www.sciencedirect.com

SCIENCE DIRECT®

Catalysis Today 88 (2004) 153–168

CATALYSIS TODAY

www.elsevier.com/locate/cattod

Mechanistic investigation of the hydrodechlorination of 1,1,1,2-tetrafluorodichloroethane on metal fluoride-supported Pt and Pd

Irmina Kris Murwani[a], Erhard Kemnitz[a,*], Tomaž Skapin[b], Mahmood Nickkho-Amiry[c], John M. Winfield[c]

[a] *Institute of Inorganic Chemistry, Humboldt University, Brook-Taylor-Str. 2, D-12489 Berlin, Germany*
[b] *Institute "Jožef Stefan", 1000 Ljubljana, Slovenia*
[c] *Department of Chemistry, University of Glasgow, Glasgow G12 8QQ, UK*

Abstract

The hydrodechlorination of CF_3CCl_2F over Pd and Pt supported on β-AlF_3 and MgF_2 with D_2 gas has been investigated employing temperature programmed isotope exchange (TPIE) under static conditions. The isotope exchange observed between the H-loaded metal catalyst and the D_2 gas phase demonstrates the significantly higher hydrogen uptake capability of Pd-based catalysts. Both Pd and Pt on β-AlF_3, show significantly higher hydrogen/deuterium uptake and isotope exchange activity as compared with the MgF_2 support, probably due to the presence of hexagonal channels in β-AlF_3 and its higher Lewis acidity. The combination of these properties make Pd/β-AlF_3 a superior catalyst for selective hydrodechlorination of CF_3CCl_2F. Based on the results of the hydrodechlorination of CF_3CCl_2F with D_2, a competitive rather than a consecutive mechanism is proposed. The data from H/D-TPIE are best interpreted by the formation of surface carbene species as intermediates.

Keywords: Hydrodechlorination of CF_3CCl_2F; Pd and Pt supported on β-AlF_3 and MgF_2; Deuterium; Temperature programmed H/D-isotope exchange; Mechanism; Surface carbene

1. Introduction

It is widely recognised that the catalytic conversion of unwanted chlorofluorocarbons (CFCs) into CFC-alternatives can be a more attractive option for their disposal than by combustion. Conversion to hydrogen containing CFC-alternatives (HFCs) is especially promising, taking into account the considerable lower potential towards ozone layer depletion of the latter. Hydrodechlorination reactions are generally catalysed by noble metals; for CFC-hydrodechlorination especially, palladium supported on high surface area materials has shown excellent activity and selectivity. The hydrodechlorination of CCl_2F_2 has been widely investigated over the past 10 years and much effort has gone into kinetic investigations [1–5]. Although direct evidence for the formation of metal-carbene species is still lacking, the results obtained suggest that this reaction occurs via a surface fluorocarbene as the reaction intermediate.

Several authors have performed hydrodechlorination reactions on CF_3CCl_2F with the aim of producing CF_3CH_2F (HFC-134a), which is an attractive

---

* Corresponding author. Tel.: +49-30-2093-7555; fax: +49-30-2093-7277.
E-mail address: erhard.kemnitz@chemie.hu-berlin.de (E. Kemnitz).

0920-5861/$ – see front matter © 2003 Elsevier B.V. All rights reserved.
doi:10.1016/j.cattod.2003.11.011

CFC-alternative. Based on conversion rates and selectivity data for this type of hydrodechlorination, a reaction mechanism which includes the intermediate formation of surface carbenes has been deduced [6–13]. For example, in order to probe the nature of the transition state to C–Cl bond cleavage, Zhou et al. [14] have established a linear free energy relationship over Pd(1 1 1) surfaces as catalysts. The intrinsic dechlorination barrier remained unchanged when the number of fluorine atoms in the reacting molecule was varied. In a very recent study, using ^{36}Cl-tracer experiments, the scission of the first C–Cl bond has been shown to be the rate determining step in the hydrodechlorination of CF_3CCl_2F [15].

Catalytic activity is influenced also by the support material. Fluoride supports should interact with hydrogen halides to a smaller extent than do oxides and among those studied are fluorides of Al [3,4,6,16–18], Ti and Zr [4] and Mg [19]. The behaviour of a deliberately, partially fluorinated alumina support has also been described [6].

Our interest has been in developing possible routes on a laboratory scale for the conversion of CFCs using heterogeneously catalysed processes, which do not require the use of anhydrous hydrogen fluoride. We studied the catalytic properties of fluorinated chromia, fluorinated alumina and β-AlF_3 [20–24] for conversion of $CClF_2CCl_2F$, via isomerisation followed by dismutation, into CF_3CCl_2F. Dehydrochlorination of the latter, forming a usable compound, CF_3CH_2F, is achieved using Pd or Pt supported on β-aluminium trifluoride or magnesium difluoride as heterogeneous catalysts [24]. This study indicated that, despite the relatively small surface areas of β-AlF_3 and MgF_2, the behaviour of fluoride-supported Pd and Pt catalysts with respect to activity and selectivity for the desired product, CF_3CH_2F, was comparable or superior to that of the carbon-supported catalysts used as benchmarks. Product distributions using very short contact times (0.3–1 s) were inconsistent with a consecutive reaction path:

$$CF_3CCl_2F \rightarrow CF_3CHClF \rightarrow CF_3CH_2F \rightarrow CF_3CH_3 \qquad (1)$$

Taken together with the observations that only low degrees of conversion were obtained using CF_3CHClF and no conversion was observed using CF_3CH_2F, it was suggested that the hydrodechlorination processes are concurrent rather than consecutive.

In the present study, we applied the temperature programmed isotope exchange (TPIE) technique [25,26] to contribute to the understanding of the mechanistic pathway of the hydrodechlorination of 1,1,1,2-tetrafluorodichloroethane.

2. Experimental

2.1. Catalyst preparation and characterisation

Magnesium fluoride and β-aluminium trifluoride were prepared according to the literature [27,28]. Their BET areas were 20.7 and 30.0 $m^2\,g^{-1}$, respectively. Following our previously described procedure [24], the support was impregnated with a 60% solution of $PdCl_2$ (Chempur, 99.99%) in 36% aqueous HCl or a 40% aqueous solution of $H_2PtCl_6\cdot6H_2O$ (Chempur) followed by drying at 393 K for 2 h. These precursors were activated by reduction at 523 K in a N_2/H_2 gas stream for 2 h and then stored in a closed container. Immediately before use, the pre-activated catalysts were again treated in the reactor at 623 K in a N_2/H_2 gas stream for at least 30 min.

Catalyst characterisation was carried out by means of XRD and BET. XRD characterisation was performed using XRD 7 Seiffert FPM (Cu Kα) equipment. Specific surface areas, S_{BET}, were determined by means of dinitrogen physisorption measured with ASAP 3000 equipment (Micromeritics). Other characterisation details of the catalysts employed for these investigations, based on temperature-programmed reduction (TPR), physi- and chemisorption using static adsorption and pulse chemisorption, respectively, transmission electron microscopy (TEM) and [^{36}Cl] studies with anhydrous HCl, have been given previously [24]. Details of the methods used for catalytic investigations under steady flow conditions have also been previously reported [20,24].

2.2. TPIE

The D/H-TPIE measurements were carried out in a quartz reactor with an on-line-coupled mass spectrometer as exemplified in Fig. 1. Before starting the

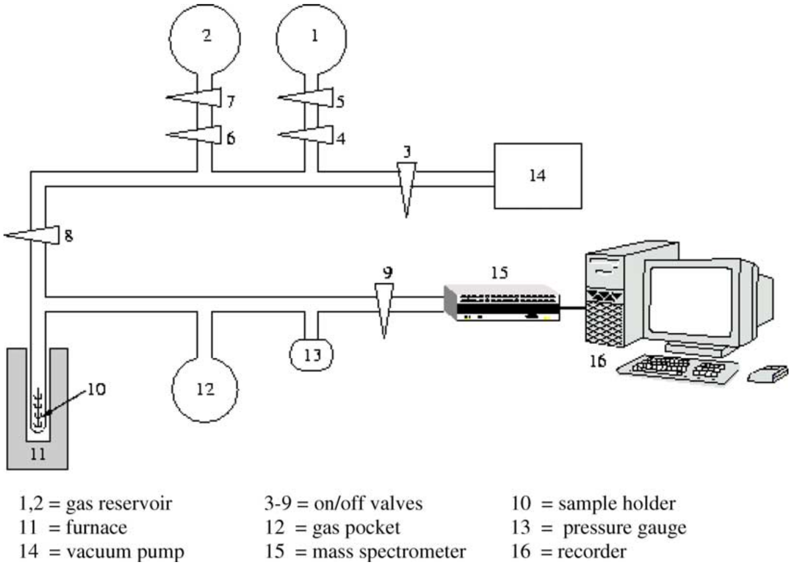

Fig. 1. The TPIE unit.

reaction, the samples (100–120 mg) were heated for 2 h at 633 K in vacuum in order to remove as much as possible of the adsorbed H_2O and H_2 from the surface of the catalyst. After cooling down to 278 K, the gases (CFC, HCFC or HFC, gifts from Solvay, purity 99% and D_2 from Messer Griesheim, purity 99.7%) were introduced into the reaction system until an initial pressure up to 120 Pa was obtained. Subsequently, the quartz reactor was heated to 633 K applying a constant heating rate of $5\,K\,min^{-1}$. The variation of the gas phase composition during constant heating was analysed by a quadrupole mass spectrometer QMG421 I (Pfeiffer Vacuum GmbH). The time lag between the sample and the MS-detector due to diffusion in the gas phase was shown in blank experiments not to exceed 4 s. This did not affect the results obtained, since the deviation was less than the uncertainty arising from the heating programme, $3\,K\,min^{-1}$, of the oven.

The raw data obtained in the measurements were evaluated utilising the manufacturer's software PROTEUS v. 4.1+ and QUADSTAR 422 v. 6.02 without further data treatment, e.g. such as smoothing.

In a given system, only very few mass numbers allow for an unequivocal decision about the presence or absence of a haloethane in the gas phase. The ions, *m*/*z* 33 (CH_2F^+), *m*/*z* 34 ($CHDF^+$), and *m*/*z* 35 (CD_2F^+) indicated the presence of CF_3CH_2F, *m*/*z* 65 ($CH_3CF_2{}^+$) and *m*/*z* 66 ($CH_2DCF_2{}^+$) were diagnostic for CF_3CH_3, *m*/*z* 135 (CF_3CClF^+) was observed from CF_3CCl_2F but not in CF_3CHClF, *m*/*z* 20 (HF^+) and *m*/*z* 21 (DF^+) indicated hydrogen fluoride and *m*/*z* 38 ($H^{37}Cl^+$) and *m*/*z* 39 ($D^{37}Cl^+$) indicated hydrogen chloride. All other fragments could have been derived from more than one compound and, hence, were used only with regard to the relative changes of the IC intensities. In Table 1 are collected extracts from the NIST library spectra of the hydrogenated halogenoethanes, together with the corresponding mass numbers of the deuterated compounds. The entries in bold type are those which permit differentiation among the various species.

For quantitative comparisons, the IC intensities of all components of the reaction system as shown in Eq. (1) were calibrated separately and these correction factors were used for the calculation of gas phase compositions.

Three types of measurements were performed:

(1) D/H isotope exchange measurements—after cooling the pretreated metal catalyst as described above, Ar and D_2 were introduced into the reaction system to give an initial partial pressure of 120 Pa (60 Pa Ar and 60 Pa D_2).

Table 1
Relevant *m*/*z* values (intensity in %) for the identification of HCFCs formed during hydrodechlorination of CFC-114a[a]

CF_3–$CFCl_2$ (CFC-114a)	CF_3–CFHCl (HCFC-124)	CF_3-CFH_2 (HFC-134a)	CF_3–CH_3 (HFC-143a)	Fragments
		33 (**100**)	33 (8)	CH_2F^+
		34 (**100**)	34 (8)	$CDHF^+$
		35 (**100**)	35 (8)	CD_2F^+ and Cl^-
	51 (52)	51 (15)		CF_2H^+
	52 (52)	52 (15)		CF_2D^+
			65 (**38**)	$CH_3CF_2{}^+$
			66 (**38**)	$CH_2DCF_2{}^+$
	67 (**100**)		**67** (**38**)	$CHClF^+$ and $CD_2HCF_2{}^+$
	68 (**100**)		**68** (**38**)	$CDClF^+$ and $CD_3CF_2{}^+$
		83 (63)		$CF_3CH_2{}^+$
		84 (63)		CF_3CDH^+
		85 (63)		$CF_3CD_2{}^+$
101 (80)	101 (40)			CCl_2F^+ and CF_3CHF^+
	102 (40)			CF_3CDF^+
135 (**100**)				CF_3CClF^+

[a] *m*/*z* fragments used for identification are marked in bold.

(2) Catalyst pretreatment in an haloethane atmosphere—the pretreated catalyst was subjected to an appropriate atmosphere (initial partial pressure of 120 Pa) and heated to 633 K in order to determine whether sorption of the substrate on the catalyst surface occurred over the temperature range of the hydrodechlorination reaction.

(3) Reaction between a haloethane and D_2—to the pretreated catalyst, a mixture of Ar, haloethane and D_2 with an overall partial pressure of 120 Pa (ratio: Ar:haloethane:D_2 = 1:1:5) was added and the reaction system heated from room temperature to 633 K.

3. Results

3.1. Catalysts

Four different catalyst systems were used in this study, derived from palladium and platinum on MgF_2 and β-AlF_3 supports. Representative catalytic data, comprehensively described and discussed already in [24], are summarised in Table 2. Under these conditions, there was no evidence that the supports, β-AlF_3 or MgF_2, behaved as catalysts for dismutation/isomerization of CCl_2FCF_3, (cf. [20]).

3.2. Catalytic activity under steady flow conditions

The Pt/MgF_2 catalyst is less selective than Pd/MgF_2, however, the latter exhibits very high selectivity towards the desired product, CF_3CH_2F (HFC-134a). The situation is even more pronounced for β-AlF_3 supports. The catalyst Pd/β-AlF_3 is both active and selective towards CF_3CH_2F formation. As can be seen from Fig. 2, the product composition changed little with variation of the contact time up to about 0.5 s, thereafter plateaux were observed.

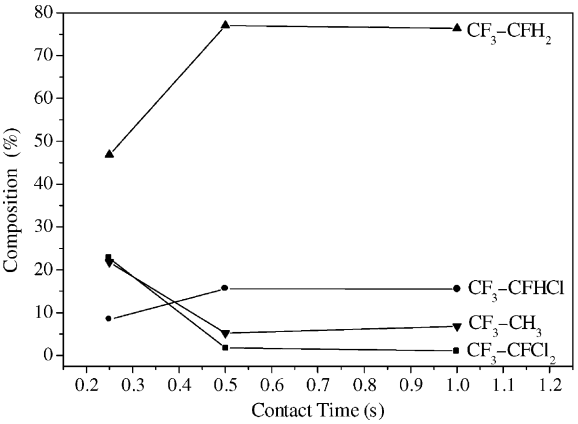

Fig. 2. Product composition from hydrodechlorination of CF_3CFCl_2 on Pd/β-AlF_3 versus contact time.

Table 2
Selected data for the conversion of CF_3Cl_2F and the selectivity of products obtained under steady flow conditions ($t_r = 1$ s, $T = 473$ K, feed ratio, $n_{H_2}/n_{CFC} = 10$)

Catalyst[a]	S_{BET} ($m^2\,g^{-1}$)[b]	Conversion (%)	Selectivity		
			CF_3CHClF	CF_3CH_2F	CF_3CH_3
Pt/MgF_2	24.0	83	52	34	14
Pd/MgF_2	27.0	92	16	74	9
Pt/β-AlF_3	32.4	30	50	30	23
Pd/β-AlF_3	30.0	97	16	79	5

[a] Nominal metal loading of the catalysts is 7.5%.
[b] S_{BET} values: $MgF_2 = 20.7\,m^2\,g^{-1}$ and β-$AlF_3 = 30.0\,m^2\,g^{-1}$.

No significant change in the conversion and product distribution was observed above this value even at 4 s (not shown here). For this reason and because of the results obtained in the earlier study [24], isotopic measurements were undertaken to probe the surface events.

3.3. TPIE measurements

In any isotopic investigation of catalytic hydrodechlorination, possible interactions between gaseous D_2 and H_2 (Eq. (2)) and between gaseous D_2 (Eqs. (3) and (4a)) or HD (Eq. (4b)) and H bonded to the metal must be considered:

$$D_{2(g)} + H_{2(g)} \rightarrow 2HD_{(g)} \quad (2)$$

$$D_{2(g)} + H_{(s)} \rightarrow HD_{(g)} + D_{(s)} \quad (3)$$

$$D_{2(g)} + 2H_{(s)} \rightarrow H_{2(g)} + 2D_{(s)} \quad (4a)$$

$$HD_{(g)} + 2H_{(s)} \rightarrow H_{2(g)} + D_{(s)} + H_{(s)} \quad (4b)$$

These processes may occur in isolation or simultaneously, depending on the nature of the compound investigated and/or the temperature. Following the approach used in the study of isotopic exchange between ^{16}O containing solid oxide and ^{18}O containing gas phase [25,26], three different coefficients derived from the measured mass spectrometric ion currents (ICs) have been calculated. They describe the partition of the hydrogen isotopes between the gas phase and the solid and, hence, allow a quantitative treatment of the experimental raw data. Their temperature dependencies can be used to differentiate among individual processes that occur simultaneously.

The coefficient, s (Eq. (5)) represents the hydrogen partial pressure of the gas phase standardised according to the hydrogen partial pressure at the beginning of the measurement ($t = 0$). The coefficient s changes only when uptake/release occurs, i.e. in-diffusion or out-diffusion processes:

$$s = \frac{\{[H_2] + [HD] + [D_2]\}_{t=i}}{\{[H_2] + [HD] + [D_2]\}_{t=0}} \quad (5)$$

An increase in s indicates a release of H_2/D_2 into the gas phase; a decrease is indicative of an uptake of H_2/D_2 by the solid or consumption due to a reaction, in the present case, hydrodechlorination.

The coefficient, c (Eq. (6)) expresses the proportion of D in the gas phase relative to the total gas phase hydrogen content. The value of c diminishes when, as a result of isotopic exchange with the solid, the deuterium content in the gas phase decreases. Both exchange and diffusion processes may be followed using this coefficient:

$$c = \frac{([HD]/2) + [D_2]}{[H_2] + [HD] + [D_2]} \quad (6)$$

The coefficient, v (Eq. (7)) represents the fraction of D in the gas phase that originates from the HD molecules:

$$v = \left\{\frac{[HD]/2}{([HD]/2) + [D_2]}\right\}_{t=i} \left\{\frac{([HD]/2) + [D_2]}{[HD]/2}\right\}_{t=0} \quad (7)$$

Any isotopic exchange resulting in the formation of HD will be reflected sensitively by v.

TPIE measurements were performed with the four catalysts, Pd supported on β-AlF_3 and MgF_2 and Pt supported on β-AlF_3 and MgF_2. Under these static

Table 3
Composition of products from hydrodechlorination of different reactants over the Pd/β-AlF_3 catalyst under static conditions at 633 K

Reactant	Conversion (%)	Product	Percentage	Compound	Selectivity (%)
CF_3–CCl_2F	23.5	CF_3CHClF	17.7	$CF_3C(H/D)ClF$	22.6
		CF_3CDClF	4.9		
		CF_3CH_2F	34.1	$CF_3C(H/D)_2F$	67.4
		CF_3CHDF	33.3		
		CF_3CH_3	9.1	$CF_3C(H/D)_3$	9.8
		CF_3CH_2D	0.7		
CF_3–$CHClF$	31.7	CF_3CH_2F	47.1	$CF_3C(H/D)_2F$	77.0
		CF_3CHDF	24.7		
		CF_3CD_2F	5.2		
		CF_3CH_3	18.1	$CF_3C(H/D)_3$	22.8
		CF_3CH_2D	4.7		
CF_3–CH_2F	3.8	CF_3CH_3	38.2	$CF_3C(H/D)_3$	100.0
		CF_3CH_2D	38.6		
		CF_3CHD_2	18.1		
		CF_3CD_3	5.1		

conditions, similar distinctive differences in catalytic activity and selectivity between Pt- and Pd-based catalysts (Tables 3 and 4) were observed. Therefore, attention will be focussed on Pd-based catalysts, representing superior behaviour as compared with Pt-based catalysts.

3.3.1. Isotope exchange between D_2 and activated Pd supported on β-AlF_3 and MgF_2

When using CF_3CFCl_2 as reactant, it is, of course, not necessary to use D_2 in the gas phase. However, for investigations using the possible consecutive products of the hydrodechlorination of CF_3CFCl_2 as reactants (cf. Eq. (1)) a knowledge of H/D-distribution may give a deeper insight into the reaction path.

Fig. 3 shows the characteristic isotope exchange behaviour of the Pd/β-AlF_3 catalyst in the absence of CF_3CCl_2F. Although the activated Pd catalyst was carefully pretreated for 2 h under high vacuum at 633 K, there was still a significant quantity of H in/on the solid catalyst. This conclusion results from the observation, made immediately after exposure to D_2 at

Table 4
Composition of products from hydrodechlorination of different reactants over the Pd/MgF_2 catalyst under static conditions at 633 K

Reactant	Conversion (%)	Product	Percentage	Compound	Selectivity (%)
CF_3CCl_2F	10.2	CF_3CHClF	5.7	$CF_3C(H/D)ClF$	7.1
		CF_3–$CDClF$	1.4		
		CF_3CH_2F	23.4	$CF_3C(H/D)_2F$	43.5
		CF_3CHDF	20.1		
		CF_3CH_3	41.5	$CF_3C(H/D)_3$	49.0
		CF_3CH_2D	7.5		
CF_3CHClF	18.2	CF_3CH_2F	42.9	$CF_3C(H/D)_2F$	71.7
		CF_3CHDF	22.9		
		CF_3CD_2F	5.9		
		CF_3CH_3	24.3	$CF_3C(H/D)_3$	28.2
		CF_3CH_2D	3.9		
CF_3CH_2F	13.4	CF_3CH_3	39.7	$CF_3C(H/D)_3$	99.8
		CF_3CH_2D	26.5		
		CF_3CHD_2	18.9		
		CF_3CD_3	14.7		

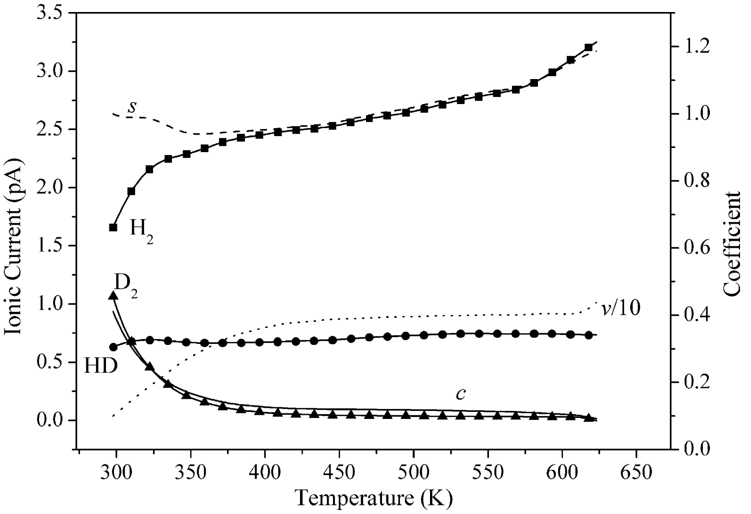

Fig. 3. IC curves for *m*/*z* 2 (H_2), *m*/*z* 3 (HD), and *m*/*z* 4 (D_2) and normalized isotope exchange coefficients for the interaction of D_2 with H_2-activated Pd/β-AlF_3.

room temperature, of nearly complete H/D-exchange, indicated by the change of the ionic currents. The *s* coefficient decreased slightly up to ca. 350 K indicating a slight uptake of hydrogen overall by the solid, and then, increased steadily with rising temperature due to an overall release of hydrogen from the solid. Therefore, in addition to the dominant process of partial heteromolecular H/D-exchange (high values of the *v* coefficient), the catalysts absorbed some hydrogen from the gas phase at low temperature. Above 350 K the increasing *s* coefficient indicated a steady release of hydrogen (predominantly as H_2). In contrast, H/D-isotope exchange on Pd/MgF_2 catalysts was suppressed at room temperature, but increased as the temperature rose (Fig. 4). This was accompanied by a sharp decrease of the *s* coefficient; the increasing

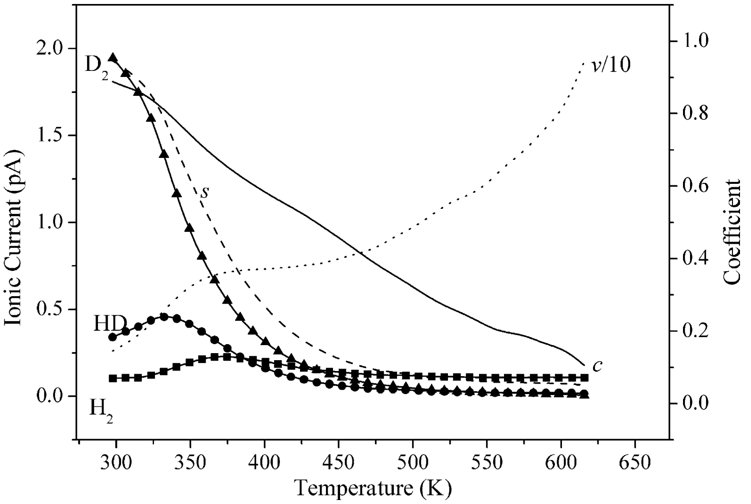

Fig. 4. IC curves for *m*/*z* 2 (H_2), *m*/*z* 3 (HD), and *m*/*z* 4 (D_2) and normalized isotope exchange coefficients for the interaction of D_2 with H_2-activated Pd/MgF_2.

v coefficient indicated a comparatively high content of HD in the gas phase remaining, as was the case for Pd/β-AlF_3. The most obvious difference between the systems was that pretreatment of Pd/MgF_2 created a catalyst which had a small quantity of hydrogen or which contained hydrogen that was not readily exchanged (strongly decreasing s coefficient), whereas Pd/β-AlF_3 still contained a significant quantity of exchangeable hydrogen. The latter resulted in facile isotope exchange with D_2. Similar differences have been found also for $H^{36}Cl$ adsorption measurements on β-AlF_3 and MgF_2 supported Pd catalysts [24] indicating the significantly higher adsorption capability of β-AlF_3 as compared with MgF_2. In separate radiotracer experiments using $H^{36}Cl$ and mass spectrometric measurements using HCl it was demonstrated that, even after careful vacuum and thermal treatment (573 K) of β-AlF_3, there were still significant amounts of water strongly bound inside the hexagonal channels of the HTB-structure of β-AlF_3. In contrast, hydrogen in MgF_2 is present only as surface hydroxyl groups, which might be easier to cleave during pretreatment [23]. Consequently, the formation of mixed hydrogen isotopic species cannot be prevented, due to water present inside the structural channels in the case of β-AlF_3 and surface hydroxyl groups in the case of MgF_2. However, this consideration does not influence greatly the results that bear on the mechanistic pathway for the hydrodechlorination of the CFC.

3.3.2. Hydrodechlorination of CF_3CCl_2F with D_2 on Pd/β-AlF_3

The temperature dependent development of product formation during hydrodechlorination of CF_3CCl_2F with D_2 is displayed in Fig. 5. Although the hydrodechlorination reaction started at comparatively low temperatures, significant conversion was observed only above ca. 425 K. This is confirmed by the change of the hydrogen isotope compositions and formation of hydrogen halides shown in Fig. 6. As can be seen from the slope of the product HCl, hydrodechlorination was observable at 325 K, but became more pronounced above 425 K. Interestingly, a comparatively constant reaction product composition was established at ca. 475 K and no significant change of this product distribution was observed above this temperature (Fig. 5). This is inconsistent with the increasing formation of HCl (Figs. 5 and 6). It may be an indication that chlorine cleaved from the organics is strongly bonded to the surface and a higher temperature is required for desorption. From a consideration of the distribution of H/D in the organic products it is concluded that (i) $CF_3CF(H/D)_2$ is formed predominantly (high selectivity towards HFC-134a) and (ii) the lighter hydrogen isotope, ^1H, is preferentially transferred into the organic compounds while ^2H (D) is more strongly bonded to the solid. This evidently indicates an isotopic effect. Fully deuterated compounds were never detected in any situation.

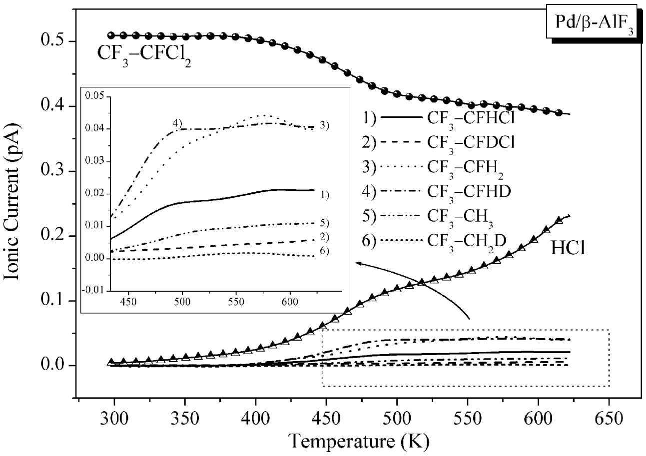

Fig. 5. IC curves for CF_3CFCl_2, $CF_3CF(H/D)Cl$, $CF_3CF(H/D)_2$, and $CF_3C(H/D)_3$ for the reaction of CF_3CFCl_2 with D_2 on H_2-activated Pd/β-AlF_3.

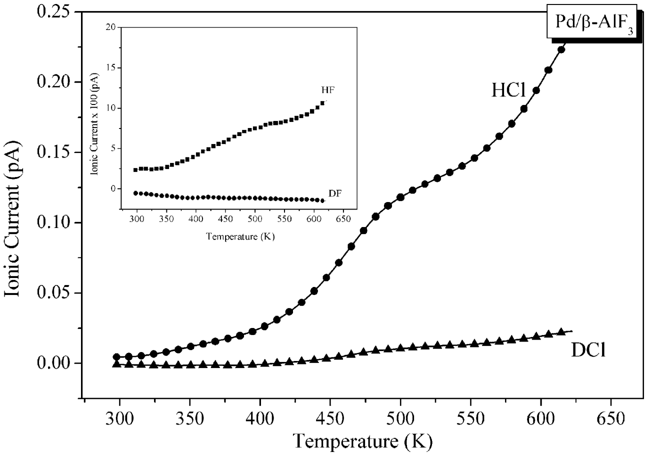

Fig. 6. IC curves for *m/z* 36.5 (HCl), *m/z* 37.5 (DCl), *m/z* 20 (HF), and *m/z* 21 (DF) for the reaction of CF_3CFCl_2 with D_2 on H_2-activated Pd/β-AlF_3.

3.3.3. Hydrodechlorination of CF_3CHClF with D_2 on Pd/β-AlF_3

The relationships between ion current values and temperature in the hydrodechlorination of CF_3CHClF with D_2 are shown in Fig. 7. From the change of the IC slopes of HCl and CF_3CH_2F (insert figure), reaction appears to commence at about 250 K but conversion is not significant until 500 K. Above this temperature the reaction markedly accelerates. As a result, the conversion of CF_3CHClF at 625 K is significantly higher compared with CF_3CCl_2F as reactant (cf. Table 3). The selectivity towards the desired product, CF_3CH_2F, is higher than with CF_3CCl_2F as reactant. H-containing products dominate over D-containing compounds.

3.3.4. Hydrodefluorination of CF_3CH_2F with D_2 on Pd/β-AlF_3

The last, unwanted, step of the reaction sequence (Eq. (1)) was examined using CF_3CH_2F as reactant (Fig. 8). As expected, this reaction was very limited but surprisingly, was observable at comparatively low temperature as indicated by the IC slope of the HF formed as the hydrodehalogenation product. Although

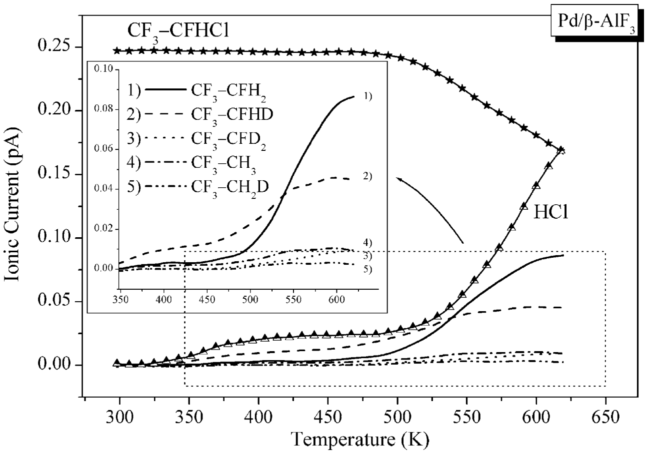

Fig. 7. IC curves for $CF_3CF(H/D)Cl$, $CF_3CF(H/D)_2$, and $CF_3C(H/D)_3$ for the reaction of $CF_3CF(H/D)Cl$ with D_2 on H_2-activated Pd/β-AlF_3.

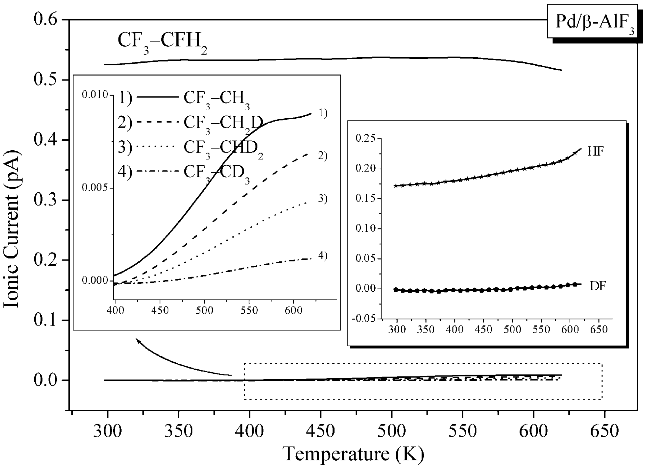

Fig. 8. IC curves for $CF_3CF(H/D)_2$, and $CF_3C(H/D)_3$ for the reaction of $CF_3CF(H/D)_2$ with D_2 on H_2-activated Pd/β-AlF_3.

very low in the absolute conversion rate, $CF_3C(H/D)_3$ formation increased above 425 K, shown from the respective IC slopes in Fig. 8 (left insert). The overall conversion at 633 K was only 3.8%, however (cf. Table 3). This finding indicates that at prolonged contact times even with HFC-134a as a reactant, hydrodefluorination may occur, unlike the situation for short contact times as in the case of steady flow conditions.

3.3.5. Hydrodechlorination of CF_3CCl_2F with D_2 on Pd/MgF_2

The IC-temperature dependencies for product formation on the Pd/MgF_2 catalyst for the three different fluorocarbons are shown in Fig. 9a–c. As for Pd/β-AlF_3, CF_3CHClF showed the highest reactivity (Fig. 9b and Table 4) and thus the highest conversion rate. The reactant, CF_3CCl_2F exhibited a continuous but slow increase in conversion with increasing temperature. The final degree of conversion determined at 633 K was approximately half that of the reactant CF_3CHClF (cf. Table 4). A surprising observation was the large quantity of CF_3CH_3 formed under these conditions resulting in a significantly lower selectivity of the Pd/MgF_2 catalyst as compared with Pd/β-AlF_3. Whereas only a low conversion of CF_3CH_2F was obtained over Pd/β-AlF_3, that over Pd/MgF_2 was higher than when using CF_3CCl_2F as reactant (Fig. 9c).

Both catalyst systems have in common the preferential formation of ^{1}H-containing organic products, whereas D is preferably bonded to the solid indicating a significant isotope effect for both catalysts.

4. Discussion

4.1. Comparisons among metal fluoride-supported Pd and Pt catalysts

A comparison of the catalytic activity of Pd and Pt supported on β-AlF_3 and MgF_2, under steady state (Table 2 and [24]) and for static conditions (Tables 3–6) indicates some common features but also obvious differences. The degree of conversion is generally significantly lower under static conditions. Since these experiments were performed under reduced partial pressure, this observation may be due mainly to the “pressure gap” under TPIE conditions. The Pt-based catalysts are generally less active compared with Pd catalysts, demonstrated by the onset temperatures for the reactions of all haloethanes used as reactants (Table 6). Most strikingly they differ in their selectivities, whereas both Pd-based catalysts exhibit very high selectivity towards CF_3CH_2F, Pt-based catalysts have very poor selectivity towards CF_3CH_2F, but fairly high selectivity towards the unwanted compound, CF_3CHClF. This difference between the metals may be rationalised on the basis of our previous observation that the H_2-uptake

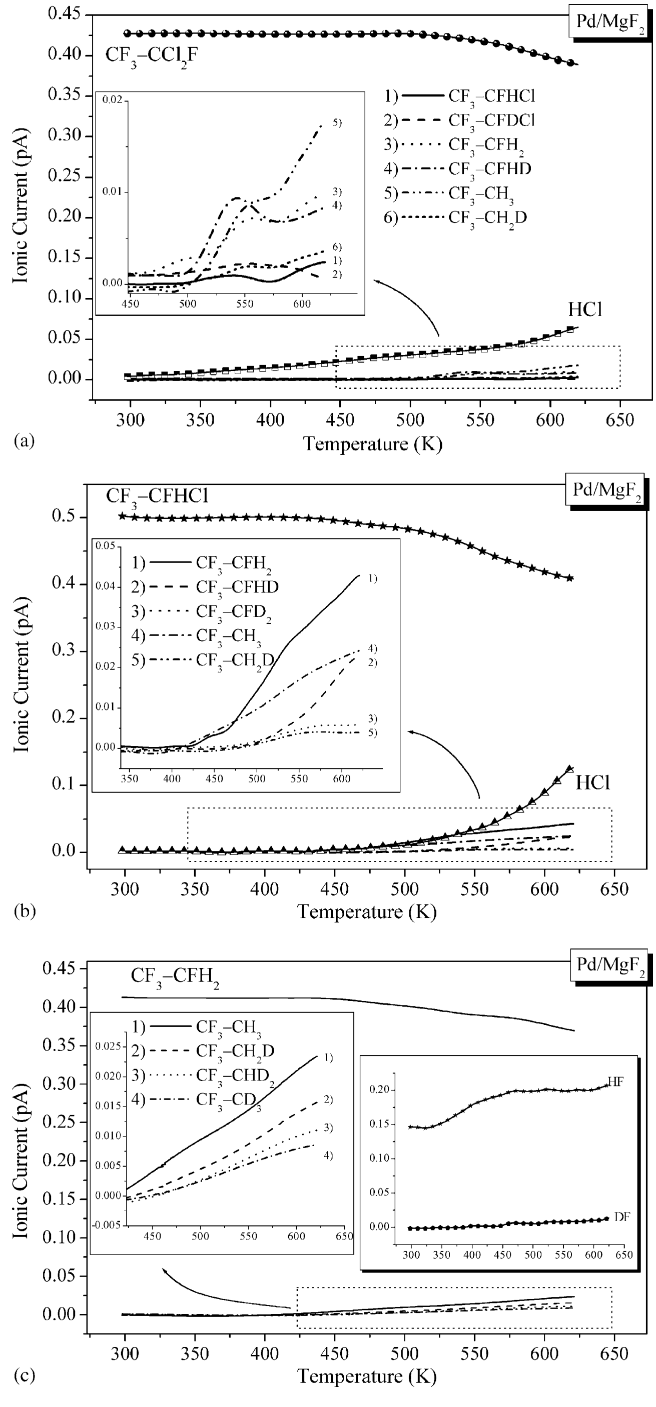

Fig. 9. IC curves for (a) CF_3CFCl_2, $CF_3CF(H/D)Cl$, $CF_3CF(H/D)_2$, and $CF_3C(H/D)_3$ for the reaction of CF_3CFCl_2 with D_2 on Pd/MgF_2; (b) $CF_3CF(H/D)Cl$, $CF_3CF(H/D)_2$, and $CF_3C(H/D)_3$ for the reaction of $CF_3CF(H/D)Cl$ with D_2 on H_2-activated Pd/MgF_2; (c) $CF_3CF(H/D)_2$ and $CF_3C(H/D)_3$ for the reaction of $CF_3CF(H/D)_2$ with D_2 on H_2-activated Pd/MgF_2.

Table 5
Gas phase composition after hydrodehalogenation at 633 K under TPIE conditions

Reactant	Conversion (%)		Product	Selectivity (%)	
	$Pt/\beta\text{-}AlF_3$	Pt/MgF_2		$Pt/\beta\text{-}AlF_3$	Pt/MgF_2
CF_3CCl_2F	8.0	12.1	$CF_3C(H/D)ClF$	62.1	54.1
			$CF_3C(H/D)_2F$	12.8	15.1
			$CF_3C(H/D)_3$	24.9	30.8
CF_3CHClF	16.8	15.1	$CF_3C(H/D)_2F$	28.7	38.4
			$CF_3C(H/D)_3$	71.3	61.6
CF_3CH_2F	0.9	5.4	$CF_3C(H/D)_3$	100.0	100.0

capability of Pd catalysts is significantly higher as compared with the Pt analogues [24]. Comparing Pd catalysts, $Pd/\beta\text{-}AlF_3$ is more reactive than Pd/MgF_2 (cf. Tables 3–6). This gradation has been found also under steady flow conditions (Table 2), although not to such a marked extent. These differences may be understood based on the experimental finding that hydrogen chemisorption was observed to occur on $Pd/\beta\text{-}AlF_3$ samples to a greater extent than on the analogous Pd/MgF_2 [24]. We believe that the strength of the Lewis acid surface sites present on the supports is also important and have previously discussed this feature of their chemistry [24].

The two catalysts also have very different isotopic exchange activities, indicating the different action of the metal fluoride supports. The first experimental point in Fig. 3 indicates that H against D isotopic exchange involving $Pd/\beta\text{-}AlF_3$ is nearly complete at about 375 K. This effect can be discussed on the basis that water is strongly bonded inside the hexagonal channels of the HTB-structure of $\beta\text{-}AlF_3$ as has been shown by us in earlier investigations of pure $\beta\text{-}AlF_3$ [23]. With increasing temperature there is a very small increase in the *s* coefficient, indicating a smooth release of small quantities of hydrogen (D/H) from the solid. The increasing *v* coefficient up to ca. 400 K indicates the formation of mixed isotopic HD due to both, isotope exchange with water (D_2/H_2O) and partial heteromolecular isotopic exchange. In contrast, the isotopic exchange behaviour of Pd/MgF_2 (Fig. 4) indicates that this catalyst does not contain easily exchangeable hydrogen. The increasing *v* coefficient over the whole temperature range measured is indicative of partial heteromolecular isotopic exchange and/or hydrogen exchange between D_2 and surface OH-groups becoming more important as the temperature increases.

Table 6
T_{onset} for the hydrodehalogenation of haloethanes over metal fluoride-supported Pd or Pt[a]

Catalyst	T_{onset} for different reactants (K)		
	CF_3CCl_2F	CF_3CHClF	CF_3CH_2F
$Pd/\beta\text{-}AlF_3$	398	338	448
Pd/MgF_2	498	448	423
$Pt/\beta\text{-}AlF_3$	448	373	573
Pt/MgF_2	373	498	448

[a] T_{onset} indicates the temperature at which the reactant IC started to change.

The isotopic exchange behaviour of Pt/metal fluoride catalysts (not shown here) differs from the Pd analogues. These catalysts are also very reactive for hydrogen isotope exchange at room temperature. However, the overall gas phase concentration of $H_2 + HD + D_2$ is significantly higher than in the Pd cases. This indicates a lower activity for isotopic exchange between D_2 and H_2O, and D_2 and surface-OH, respectively, which may explain the lower activity towards the formation of the more highly hydrogenated compounds, CF_3CH_2F and CF_3CH_3 (Tables 3–5).

4.2. Carbene versus consecutive mechanism

Since a D against H exchange could not be excluded due to the presence of structural water in case of the $\beta\text{-}AlF_3$ and of surface OH-groups in case of MgF_2 supports, the distribution of the differently deuteriated products cannot be discussed in detail. A quantitative consideration of the differently deuterated HCFCs indicates an approximate correspondence to the distribution of D and H isotopes in the starting gas phase. Hence, all isotopomers of each compound are considered as a group.

Although a consecutive hydrodechlorination reaction mechanism is possibly the most obvious, it should result in significant product distribution change with change in contact time. This has not been observed [24] (cf. Fig. 2). Moreover, the product distribution (selectivity) determined under static gas phase but dynamic thermal conditions does not change greatly up to ca. 500 K (Figs. 5 and 9a). It should be born in mind that the temperature scale represents also a time scale because the temperature increase was programmed (5 K min^{-1}). Hence temperature dependence also indicates reaction time dependence. This also argues strongly against a consecutive reaction pathway although all these data represent cumulative data under the experimental conditions chosen here.

Fig. 10 shows the absolute yields of products over the Pd/β-AlF_3 catalyst obtained using the three possible reactants, CF_3CCl_2F, CF_3CClHF, and CF_3CH_2F. The most obvious inconsistency, when a consecutive mechanism is proposed, concerns the content of CF_3CH_3 (HFC-143a) formed using (i) CF_3CHClF and (ii) CF_3CH_2F as reactants. In both experiments, the same partial pressure of reactants was used. In the case of CF_3CHClF as reactant, about 7% CF_3CH_3 was formed. For a consecutive reaction, the limiting concentration should be the amount of CF_3CH_2F formed from CF_3CHClF. The proportion of CF_3CH_2F is about 24% of the overall gas phase composition, therefore the mole ratio of CF_3CH_2F to CF_3CH_3 is about 3:1. Starting from CF_3CH_2F should result in at least the same relative amount of the only possible product, CF_3CH_3, whose proportion should be about 25%. In reality, only 4% CF_3CH_3 is formed under these conditions.

The most probable alternative is a carbene mechanism. Carbenes readily undergo coupling reactions and addition to saturated or unsaturated molecules. Reactions of carbenes with olefins typically yield products formed through the addition of the carbene to the olefin double bond [29]. Thus, Deshmukh and d'Itri [11] proved indirectly the presence of CF_2 and CH_2 carbenes as intermediates in the hydrodechlorination reaction of CF_2Cl_2 by addition of pulses of C_2H_4 to the reaction gas stream which gave a small but detectable amount of propane.

In the present work, the compounds in the reaction system (Eq. (1)) can be represented by the general formula $RCF(X/Y)_2$, where $R = CF_3$, $X = Cl$ and $Y = H$. The chemically inert CF_3 group is almost as electronegative as fluorine. Formation of a carbene, hence, is unlikely to involve the CF_3 group directly but could involve scission of either a C–Cl (254 kJ mol^{-1}), a C–H (439 kJ mol^{-1}) or a C–F bond (460 kJ mol^{-1}) [30]. Scission of a C–Cl bond should occur preferentially; scission of a C–F bond is the most energy demanding and thus, less likely. Carbenes of the general composition, RR′C:, should be stabilised by electronegative groups or atoms, R and R′. Thus, the carbenes that could be derived from CF_3CCl_2F, ordered according to decreasing stability, are CF_3CF :>

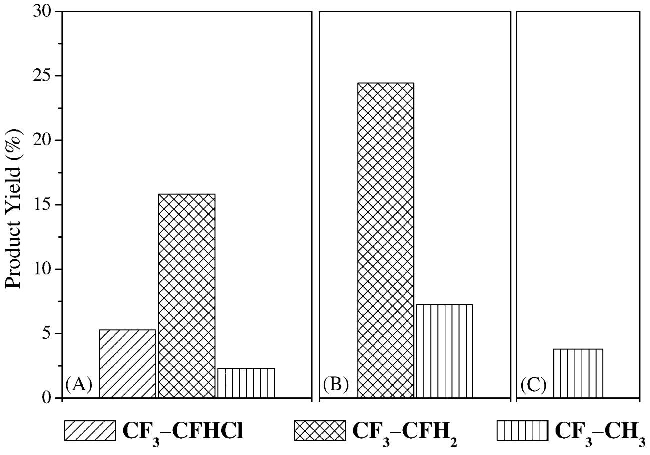

Fig. 10. Product yields for hydrodechlorination starting with: (A) CF_3CFCl_2, (B) CF_3CFHCl, and (C) CF_3CFH_2 on H_2-activated Pd/β-AlF_3.

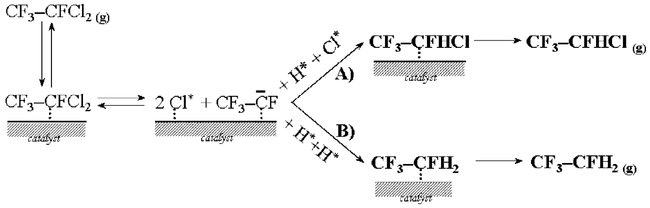

Scheme 1.

CF_3CCl :> CF_3CH :. One would expect the formation of the carbene CF_3CF: when starting with CF_3CCl_2F. Surprisingly, however, CF_3CHClF, from which the obvious carbene is also CF_3CF:, is significantly more reactive than CF_3CHCl_2. The most probable explanation for this finding may be an additional driving force due to the formal formation of HCl ($H_{(ad)}$ plus $Cl_{(ad)}$). The low reactivity of CF_3CH_2F follows the prediction made from the order given above. Since the surface species were not identified, this discussion is speculative.

In order to attempt to obtain more definitive evidence, in recent work the PulseTA® technique, coupled with mass spectrometry, has been applied to the reactive interaction of a Pd/β-AlF_3 catalyst with CF_3CCl_2F [31]. By reducing the Pd/β-AlF_3 precursor with hydrazine instead of hydrogen gas, catalyst totally free of hydrogen could be obtained. Although this method is very sensitive, no indication for any kind of reactive interaction between the catalyst and pure CF_3CCl_2F was found. However, when D_2 alone or D_2 together with CF_3CCl_2F were pulsed, an unambiguous detection of an interaction with the solid was possible [31]. The conclusion is that any carbenes formed must have very short lifetimes.

It is concluded that a very labile equilibrium between CF_3CCl_2F and a surface carbene is followed by removal of the latter to give CF_3CHClF and CF_3CH_2F (Scheme 1).

Under conditions where the catalyst provides a high surface concentration of activated hydrogen, as demonstrated for Pd/β-AlF_3, path B is the dominating process. Under these conditions the relative surface concentration of activated Cl is comparatively low and reaction path A in Scheme 1 is suppressed. On this basis, the unusual relationships of the product distributions with increasing contact time (Fig. 2) can be rationalised. Path A requires the surface carbene to have a longer life time in order for its reaction with surface H and Cl to occur. A contact time of 0.3 s is obviously sufficient for both pathways to be observed (Fig. 2). However using the PulseTA® technique [31], the contact time of 0.02 s, was apparently too short to detect the last step of reaction path A in Scheme 1,

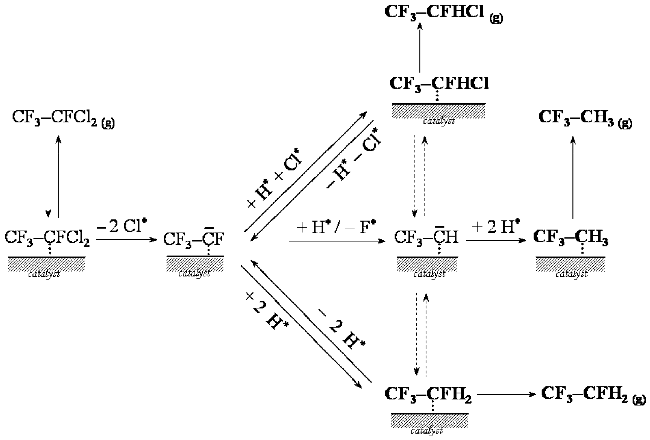

Scheme 2.

that means no conversion of CF_3CFH_2 into CF_3CH_3 was observed under these conditions. The overall reaction mechanism may be described according to Scheme 2, which is an extension of that proposed for CF_2Cl_2 [11].

A carbene-like surface species may be formed but there is no evidence that it exists in the free state. It appears to be the most important surface intermediate, however, and can react to give either CF_3CHClF or CF_3CH_2F. Since the C–F bond is very strong, only at elevated temperature does limited scission of this bond occur since only low conversion into CF_3CH_3 is observed when starting with CF_3CH_2F.

This hypothetical mechanism is supported also by the differences found in the behaviour of the metal fluoride supports. β-AlF_3 is known to be a reasonably strong Lewis acid; the surface Al-sites are the sites for adsorptive activation of fluorochlorocarbons [32]. In contrast, MgF_2 is a very weak Lewis acid [33,34] and is not suitable for activation of fluorochlorocarbons. Hence, the β-AlF_3 support directly enhances the adsorption of the halocarbon near to the metal catalyst. Additionally, any carbene formed at the catalyst surface should be stabilised by an electron withdrawing Lewis acid. This property is likely to be a factor in increasing the activity of the Pd/β-AlF_3 catalyst.

5. Conclusion

Palladium-based catalysts are significantly more selective than Pt for the hydrodechlorination of CF_3CCl_2F to form the useful compound CF_3CH_2F. This is due mainly to a bigger pool of activated surface hydrogen species. The greater Lewis acidity of β-AlF_3 compared with MgF_2 is also important. Hence, the halocarbon activation and subsequent hydrogenolysis occurs more effectively on Pd/β-AlF_3 than on Pd/MgF_2. As a result, Pd/β-AlF_3 has a similar activity but an higher selectivity towards CF_3CH_2F formation than Pd/charcoal, even although the surface area of the latter support is two orders of magnitude larger [24].

The different rates of the reactions that involve surface carbene-like species are the key in determining the observed selectivity. Since the most probable surface intermediate, CF_3CF:, reacts with one H and one Cl surface atoms, forming CF_3CHClF, more slowly than with two surface hydrogen atoms, selectivity towards the formation of CF_3CH_2F on Pd/β-AlF_3 is observed. The last step, formation of the hydrogen containing surface carbene CF_3CH: originating from an H-for-F exchange in the primary carbene CF_3CF:, is an energy demanding process and, hence, less probable. Therefore, the formation of CF_3CH_3 becomes more dominant only at elevated temperatures.

References

[1] B. Coq, J.M. Cognion, F. Figueras, D. Tornigant, J. Catal. 141 (1993) 21.
[2] Z. Karpinski, K. Early, J.L. d'Itri, J. Catal. 164 (1996) 378.
[3] E.J.A.X. van de Sandt, A. Wiersma, M. Makkee, H. van Bekkum, J.A. Moulijn, Appl. Catal. A 155 (1997) 57.
[4] B. Coq, J.M. Cognion, S. Hub, D. Tornigant, J. Phys. Chem. 99 (1995) 1115.
[5] E.J.A.X. van de Sandt, A. Wiersma, M. Makkee, H. van Bekkum, J.A. Moulijn, Catal. Today 27 (1996) 257.
[6] K. Early, V.I. Kovalchuk, F. Lonyi, S. Desmukh, J. d'Itri, J. Catal. 182 (1999) 219.
[7] C.D. Thompson, R.M. Rioux, N. Chen, F.H. Ribeiro, J. Phys. Chem. B 104 (2000) 3067.
[8] F.H. Ribeiro, C.A. Gerken, G.A. Somorjai, C.S. Kellner, G.W. Coulston, L.E. Manzer, L. Abrams, Catal. Lett. 45 (1997) 149.
[9] P. Bodnariuk, B. Coq, G. Ferrat, F. Figueras, J. Catal. 116 (1989) 459.
[10] B. Coq, G. Ferrat, F. Figueras, J. Catal. 101 (1986) 434.
[11] S. Deshmukh, J. d'Itri, Catal. Today 40 (1998) 377.
[12] E.J.A.X. van de Sandt, A. Wiersma, M. Makkee, H. van Bekkum, J.A. Moulinjn, Recl. Trav. Chim. Pays-Bas 115 (1996) 505.
[13] M.T. Buelow, B. Immaraporn, A.J. Gellman, J. Am. Chem. Soc. 123 (2001) 1440.
[14] G. Zhou, Ch. Chan, A.J. Gellmann, J. Phys. Chem. B 103 (1999) 1134.
[15] N. Chen, R.B. Rioux, F.H. Ribeiro, J. Catal. 211 (2002) 192.
[16] B. Coq, J.M. Cognion, F. Figuéras, D. Tournigant, J. Catal. 141 (1993) 21.
[17] B.S. Ahn, S.C. Lee, D.J. Moon, B.G. Lee, J. Mol. Catal. A 106 (1996) 83.
[18] D.J. Moon, M.J. Chung, K.Y. Park, S.I. Hong, Appl. Catal. A 168 (1998) 159.
[19] A. Malinowski, W. Juszczyk, J. Pielaszek, M. Bonarowska, M. Wojciechowska, Z. Karpiński, J. Chem. Soc., Chem. Commun. (1999) 685.
[20] H. Bozorgzadeh, E. Kemnitz, M. Nickkho-Amiry, T. Skapin, J.M. Winfield, J. Fluor. Chem. 107 (2001) 45.
[21] H. Bozorgzadeh, E. Kemnitz, M. Nickkho-Amiry, T. Skapin, J.M. Winfield, J. Fluor. Chem. 110 (2001) 181.

[22] H. Bozorgzadeh, E. Kemnitz, M. Nickkho-Amiry, T. Skapin, G.D. Tate, J.M. Winfield, J. Fluor. Chem. 112 (2001) 225.

[23] C.H. Barclay, H. Bozorgzadeh, E. Kemnitz, M. Nickho-Amiry, D.E.M. Ross, T. Skapin, J. Thomson, G. Webb, J.M. Winfield, J. Chem. Soc., Dalton Trans. (2002) 40.

[24] H. Berndt, H. Bozorgzadeh, E. Kemnitz, M. Nickkho-Amiry, M.-M. Pohl, T. Skapin, J.M. Winfield, J. Mater. Chem. 12 (2002) 3499.

[25] E. Kemnitz, C. Stöcker, T. Olesch, D.-H. Menz, Thermochim. Acta 225 (1993) 119.

[26] A.A. Galkin, G.N. Mazo, A.P. Mozhaev, S. Scheurell, E. Kemnitz, Solid State Ionics 101–103 (1997) 1087.

[27] M. Wojciechowska, K. Novinska, W. Kania, A. Nowacka, React. Kinet. Catal. Lett. 2 (1975) 229.

[28] D.-H. Menz, U. Bentrup, Z. Anorg. Allg. Chem. 576 (1989) 186.

[29] W. Kirmse, Carbene Chemistry, 2nd ed., Academic Press, New York, 1971, pp. 267ff.

[30] P.J. Chupas, M.F. Ciraolo, J.C. Hanson, C.P. Grey, J. Am. Chem. Soc. 123 (2001) 1694.

[31] M. Feist, I.K. Murwani, E. Kemnitz, J. Therm. Anal. Cal. 72 (2003) 75, 82.

[32] A. Hess, E. Kemnitz, A. Lippitz, W.E.S. Unger, D.-H. Menz, J. Catal. 148 (1994) 270.

[33] M. Wojciechowska, Bull. Acad. Pol. Chim. 29 (1981) 533.

[34] E. Kemnitz, A. Hess, G. Rother, S.I. Troyanov, J. Catal. 159 (1996) 332.